

LOW-COMPLEXITY MIMO-BICM RECEIVERS WITH IMPERFECT CHANNEL STATE INFORMATION: CAPACITY-BASED PERFORMANCE COMPARISON

Clemens Novak and Gerald Matz

Institute of Communications and Radio-Frequency Engineering, Vienna University of Technology
Gusshausstrasse 25/389, A-1040 Vienna, Austria; e-mail: clemens.novak@tuwien.ac.at

ABSTRACT

This paper provides a performance comparison of soft MMSE and max-log demodulators for multiple-input multiple-output (MIMO) bit-interleaved coded modulation (BICM) systems with imperfect channel state information. We use the capacity of the equivalent modulation channel as a code-independent performance metric. Our results show that the conventional approach of mismatched demodulation is noticeably inferior to optimal demodulators that are derived by conditioning on the channel estimate right from the beginning. Numerical simulations further demonstrate the importance of appropriate pilot power allocation.

1. INTRODUCTION

1.1. Background

Bit-interleaved coded modulation (BICM) is a promising scheme for multiple-input multiple-output (MIMO) wireless systems [1, 2]. With BICM, a block of information bits is mapped to transmit symbols via a channel encoder and a symbol mapper which are separated by an interleaver. At the receiver, a soft-output demodulator calculates *log-likelihood ratios* (LLR) for the code bits, which are deinterleaved and passed to the channel decoder. Since MAP and max-log demodulation in MIMO-BICM systems are computationally expensive, many low-complexity demodulators have been proposed in the literature. It was recently demonstrated [3] that the performance of the soft MMSE demodulator proposed in [4] is close to optimal for many system configurations and operating regimes.

Soft-output demodulators for MIMO-BICM are usually designed assuming perfect channel state information (CSI). In practice, CSI is obtained via pilot symbol assisted channel estimation. Estimation errors result in imperfect CSI that causes conventional MIMO demodulators to be mismatched and thereby deteriorates their performance significantly. Demodulation in MIMO systems with imperfect CSI has been first addressed in [5]. Taking into account the statistics of the channel estimate, an optimal version of the max-log demodulator has been proposed in [6]. Its performance in the context of iteratively decoded MIMO-BICM was investigated in [7] by means of EXIT charts. In a similar spirit, a modified

soft MMSE demodulator using CSI statistics has been presented [8]; its performance was verified in terms of bit error rate (BER) using an off-the-shelf LDPC code.

1.2. Contributions

The novel aspects of this work can be summarized as follows:

- By extending the optimal soft MMSE demodulator [8] to arbitrary linear channel estimators, we show that the optimal soft MMSE demodulator is actually independent of the specific linear channel estimator used.
- Following [3], we assess the performance of mismatched and optimal demodulators under imperfect CSI using the mutual information of the equivalent modulation channel. This mutual information can be interpreted as maximum achievable information rate and provides a code-independent performance metric.
- We compare the maximum achievable rates of mismatched and optimal soft MMSE receivers for correlated and uncorrelated MIMO channels. As baseline systems, we use the rates achievable with the mismatched and optimal max-log demodulator, and the maximum achievable rates of demodulators with perfect CSI.
- We investigate how the allocation of power to data and pilots impacts the maximum achievable rate, thereby revealing the importance of optimal power allocation.

The paper is organized as follows. In Section 2 we introduce the system model. Channel estimation and the various demodulator designs are discussed in Section 3. Section 4 proposes to assess demodulator performance in terms of system capacity. In Section 5 we present our numerical results. Section 6 provides conclusions.

2. SYSTEM MODEL

Fig. 1 shows a block diagram of the MIMO-BICM system considered. There are M_T antennas at the transmitter and M_R antennas at the receiver. The MIMO-BICM transmitter first encodes a length- K sequence of information bits $\mathbf{b} = (b_1 \dots b_K)^T$ into a length- M sequence of code bits by means of a channel code (thus, the code rate equals $R = K/M$). The code bits are passed through a bitwise interleaver Π . The resulting sequence of interleaved code bits $\mathbf{d} = (d_1 \dots d_M)^T$ is scrambled by a pseudo-random sequence \mathbf{q} . The uniformly distributed, interleaved, and scrambled code bits are

This work was funded by the FWF project "Information Networks" (Grant No. S10606) within the National Research Network SISE and by the Network of Excellence NEWCOM++ (IST-216715).

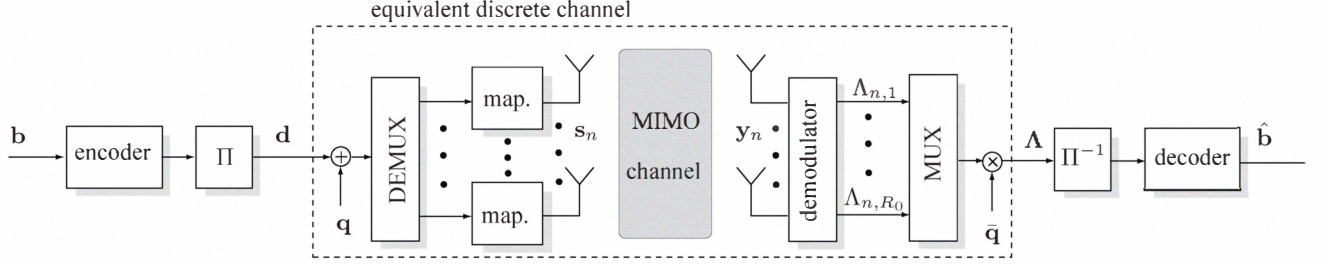


Fig. 1. Block diagram of a MIMO-BICM system.

demultiplexed into M_T antenna streams (“layers”). In each layer $k = 1, \dots, M_T$, groups of B successive bits $\mathbf{d}_{n,k} = (d_{l(n)+(k-1)B+1} \dots d_{l(n)+kB})^T$, with $l(n) = (n-1)M_TB$ are mapped to symbols $s_{n,k}$ from a symbol alphabet \mathcal{A} of size $|\mathcal{A}| = 2^B$ and mean power $E_s \triangleq \frac{1}{|\mathcal{A}|} \sum_{a \in \mathcal{A}} |a|^2$. The transmit vector at symbol time n is given by $\mathbf{s}_n \triangleq (s_{n,1} \dots s_{n,M_T})^T$ and carries $R_0 \triangleq BM_T$ interleaved code bits \mathbf{d}_n .

Assuming block flat fading, the length- M_R receive vector at symbol time n is given by

$$\mathbf{y}_n = \mathbf{H}\mathbf{s}_n + \mathbf{w}_n, \quad n = 1, \dots, N. \quad (1)$$

Here, \mathbf{H} denotes the $M_R \times M_T$ MIMO channel matrix, $\mathbf{w}_n \sim \mathcal{CN}(\mathbf{0}, \sigma_w^2 \mathbf{I})$ denotes i.i.d. complex Gaussian noise, and $N = M/(BM_T)$ is the block length. By stacking the columns of the channel matrix \mathbf{H} into a vector $\mathbf{h} = \text{vec}\{\mathbf{H}\}$ and defining $\mathbf{S}_n = \mathbf{s}_n^T \otimes \mathbf{I}$, (1) can be rewritten as

$$\mathbf{y}_n = \mathbf{S}_n \mathbf{h} + \mathbf{w}_n, \quad n = 1, \dots, N. \quad (2)$$

The channel vector \mathbf{h} is assumed zero-mean complex Gaussian with covariance matrix \mathbf{C}_h , $\mathbf{h} \sim \mathcal{CN}(\mathbf{0}, \mathbf{C}_h)$.

For channel estimation, the pilot vector sequence $\mathbf{p}_1, \dots, \mathbf{p}_{N_p}$ of length $N_p \geq M_T$ is transmitted during a training phase. We define $\mathbf{P} = (\mathbf{P}_1^T \dots \mathbf{P}_{N_p}^T)^T$ with $\mathbf{P}_n = \mathbf{p}_n^T \otimes \mathbf{I}$ and assume orthogonal training sequences, i.e., $\mathbf{P}^H \mathbf{P} = N_p \mathbf{I}$. The total training power is $E_p \triangleq N_p P$. The received pilot sequence vector of length $N_p M_R$ equals

$$\tilde{\mathbf{y}}_p = \mathbf{P}\mathbf{h} + \tilde{\mathbf{w}},$$

with the length- $N_p M_R$ noise vector $\tilde{\mathbf{w}} \sim \mathcal{CN}(\mathbf{0}, \sigma_w^2 \mathbf{I})$.

3. MIMO-BICM WITH IMPERFECT CSI

The receiver structure employed is shown in Fig. 1 and consists basically of a demodulator and a channel decoder. The demodulator calculates bit LLRs which are descrambled by the sequence $\bar{\mathbf{q}} = 1 - 2\mathbf{q}$, deinterleaved, and then passed to the channel decoder. The decoder finally obtains decisions for the information bits. In addition, a channel estimator (not shown in Fig. 1) provides an estimate $\hat{\mathbf{H}}$ of the channel based on $\tilde{\mathbf{y}}_p$ and the known training matrix \mathbf{P} .

3.1. Channel Estimation

LS and MMSE Estimator [9]. An estimate of the channel matrix is obtained according to $\hat{\mathbf{H}} = \text{unvec}\{\hat{\mathbf{h}}\}$ with

$$\hat{\mathbf{h}} = \mathbf{A}\tilde{\mathbf{y}}_p = \mathbf{A}(\mathbf{P}\mathbf{h} + \tilde{\mathbf{w}}). \quad (3)$$

Here, \mathbf{A} is a $M_T M_R \times N_p M_R$ full-rank estimator matrix.

With our assumption of orthogonal training sequences, the LS channel estimate simply reads $\hat{\mathbf{h}}_{\text{LS}} = \frac{1}{E_p} \mathbf{P}^H \tilde{\mathbf{y}}_p$. An alternative is provided by the MMSE estimate which equals

$$\hat{\mathbf{h}}_{\text{MMSE}} = \frac{1}{\sigma_w^2} \Sigma \mathbf{P}^H \tilde{\mathbf{y}}_p, \quad \text{with } \Sigma = \left(\mathbf{C}_h^{-1} + \frac{E_p}{\sigma_w^2} \mathbf{I} \right)^{-1}.$$

Posterior Channel Distribution. We next determine the posterior density $f(\mathbf{h}|\hat{\mathbf{h}})$ of the channel \mathbf{h} given the estimate $\hat{\mathbf{H}}$. Since \mathbf{h} and $\tilde{\mathbf{w}}$ are independent and Gaussian, (3) implies that $\mathbf{z} = \begin{pmatrix} \mathbf{h} \\ \hat{\mathbf{h}} \end{pmatrix} \sim \mathcal{CN}(\mathbf{0}, \mathbf{C}_z)$ is Gaussian with covariance

$$\mathbf{C}_z = \begin{pmatrix} \mathbf{C}_h & \mathbf{C}_{h,\hat{h}}^H \\ \mathbf{C}_{\hat{h},h} & \mathbf{C}_{\hat{h}} \end{pmatrix},$$

where $\mathbf{C}_{\hat{h},h} = \mathbf{A}\mathbf{P}\mathbf{C}_h$ and $\mathbf{C}_{\hat{h}} = \mathbf{A}\mathbf{P}\mathbf{C}_h\mathbf{P}^H\mathbf{A}^H + \sigma_w^2 \mathbf{A}\mathbf{A}^H$.

This furthermore implies [9] that conditional on $\hat{\mathbf{h}}$ the channel \mathbf{h} is also Gaussian with conditional mean equal to the MMSE estimate $\mu_{h|\hat{h}} = \mathbf{C}_{h,\hat{h}}\mathbf{C}_{\hat{h}}^{-1}\hat{\mathbf{h}}$ and conditional covariance given by the Schur complement of $\mathbf{C}_{\hat{h}}$, i.e., $\mathbf{C}_{h|\hat{h}} = \mathbf{C}_h - \mathbf{C}_{\hat{h},h}^H \mathbf{C}_{\hat{h}}^{-1} \mathbf{C}_{\hat{h},h}$. Invoking the assumptions that \mathbf{P} is orthogonal and \mathbf{A} has full rank, we obtain after some algebra $\mu_{h|\hat{h}} = \hat{\mathbf{h}}_{\text{MMSE}}$ and $\mathbf{C}_{h|\hat{h}} = \Sigma$ and hence

$$\mathbf{h}|\hat{\mathbf{h}} \sim \mathcal{CN}(\hat{\mathbf{h}}_{\text{MMSE}}, \Sigma). \quad (4)$$

We emphasize that this result holds true for *any* linear estimator (cf. (3)) provided the estimator matrix \mathbf{A} has full rank.

3.2. Genie and Mismatched Demodulation

From now on, we will drop the symbol time index n to simplify notation. Assuming perfect CSI, the optimal demodulator calculates the posterior likelihood ratios (LLR) of the

BM_T bits d_k according to

$$\Lambda_k \triangleq \log \frac{P(d_k = 1|\mathbf{y}, \mathbf{H})}{P(d_k = 0|\mathbf{y}, \mathbf{H})} = \log \frac{\sum_{\mathbf{s} \in \chi_k^1} f(\mathbf{y}|\mathbf{s}, \mathbf{H})}{\sum_{\mathbf{s} \in \chi_k^0} f(\mathbf{y}|\mathbf{s}, \mathbf{H})} \quad (5)$$

$$\approx \min_{\mathbf{s} \in \chi_k^0} \frac{1}{\sigma_w^2} \|\mathbf{y} - \mathbf{H}\mathbf{s}\|^2 - \min_{\mathbf{s} \in \chi_k^1} \frac{1}{\sigma_w^2} \|\mathbf{y} - \mathbf{H}\mathbf{s}\|^2. \quad (6)$$

The last expression, obtained via the max-log approximation, will be referred to as *genie max-log* demodulator. The conventional approach to deal with imperfect CSI, termed *mismatched max-log* demodulation, replaces \mathbf{H} in (6) with $\hat{\mathbf{H}}$.

Since max-log demodulation tends to be computationally expensive, [4] proposed a soft demodulator based on (linear) MMSE equalization and *per-layer* max-log LLR calculation. The MMSE equalizer output is given by

$$\hat{\mathbf{s}}^{\text{MMSE}} = \mathcal{E}\{\mathbf{s}\mathbf{y}^H|\mathbf{H}\} (\mathcal{E}\{\mathbf{y}\mathbf{y}^H|\mathbf{H}\})^{-1} \mathbf{y} = \mathbf{W}\mathbf{y} \quad (7)$$

with the Wiener filter

$$\mathbf{W} = \mathbf{H}^H \left(\mathbf{H}\mathbf{H}^H + \frac{\sigma_w^2}{E_s} \mathbf{I} \right)^{-1}. \quad (8)$$

Assuming that the residual interference at the equalizer output is Gaussian, the approximate LLR for the i th bit in layer l is subsequently computed according to

$$\Lambda_{l,i}^{\text{MMSE}} = \frac{1}{\sigma_l^2} \left[\min_{s \in \mathcal{A}_i^0} |\hat{s}_l^{\text{MMSE}} - \mu_l s|^2 - \min_{s \in \mathcal{A}_i^1} |\hat{s}_l^{\text{MMSE}} - \mu_l s|^2 \right].$$

Here $\mu_l = [\mathbf{W}\mathbf{H}]_{l,l}$, $\sigma_l^2 = \mu_l - \mu_l^2$, and \mathcal{A}_i^b denotes the set of transmit symbols, whose bit label at position i equals b . The *genie MMSE* demodulator just described assumes perfect CSI. Practical implementations use a *mismatched MMSE* demodulator in which the true channel \mathbf{H} in (8) is replaced with a channel estimate $\hat{\mathbf{H}}$. We note that the performance of mismatched max-log and MMSE demodulation depends critically on the actual channel estimate.

3.3. Optimal Demodulators

The mismatched demodulators do not exploit the statistical information about \mathbf{h} conveyed by the channel estimate $\hat{\mathbf{h}}$ according to (4). Rather than replacing \mathbf{H} with $\hat{\mathbf{H}}$ in the final results (6) and (8), this replacement should be made right in the beginning, i.e., the conditioning in (5) and (7) should be with respect to $\hat{\mathbf{H}}$ instead of \mathbf{H} . Using the relation

$$f(\mathbf{y}|\mathbf{s}, \hat{\mathbf{H}}) = \int f(\mathbf{y}|\mathbf{s}, \mathbf{H}) f(\mathbf{H}|\hat{\mathbf{H}}) d\mathbf{H},$$

and the Gaussianity of the densities involved, we obtain

$$\mathbf{y}|\mathbf{S}, \hat{\mathbf{H}} \sim \mathcal{CN}(\hat{\mathbf{H}}_{\text{MMSE}}\mathbf{S}, \mathbf{S}\Sigma\mathbf{S}^H + \sigma_w^2\mathbf{I}),$$

with $\hat{\mathbf{H}}_{\text{MMSE}} = \text{unvec}\{\hat{\mathbf{h}}_{\text{MMSE}}\}$ (see Section 3.1). This distribution is again independent of the actual channel estimator used and leads to an *optimal max-log* demodulator that replaces $\frac{1}{\sigma_w^2} \|\mathbf{y} - \mathbf{H}\mathbf{s}\|^2$ in (6) with the metric

$$(\mathbf{y} - \hat{\mathbf{H}}_{\text{MMSE}}\mathbf{s})^H (\Sigma_{\mathbf{s}} + \sigma_w^2\mathbf{I})^{-1} (\mathbf{y} - \hat{\mathbf{H}}_{\text{MMSE}}\mathbf{s}) - \log \det (\Sigma_{\mathbf{s}} + \sigma_w^2\mathbf{I})$$

with $\Sigma_{\mathbf{s}} = (\mathbf{s}^T \otimes \mathbf{I}) \Sigma (\mathbf{s} \otimes \mathbf{I})$. This differs from the mismatched max-log demodulator in that the appropriate covariance matrix $\Sigma_{\mathbf{s}} + \sigma_w^2\mathbf{I}$ is used instead of $\sigma_w^2\mathbf{I}$ and in that there is the additional log-det term that depends on the symbols.

In a similar spirit, [8] proposed an *optimal soft MMSE* demodulator given by

$$\tilde{\mathbf{s}}^{\text{MMSE}} = \mathcal{E}\{\mathbf{s}\mathbf{y}^H|\hat{\mathbf{H}}\} (\mathcal{E}\{\mathbf{y}\mathbf{y}^H|\hat{\mathbf{H}}\})^{-1} \mathbf{y} = \tilde{\mathbf{W}}\mathbf{y}. \quad (9)$$

Using (1) and (4), it is straightforward to show that the modified Wiener filter $\tilde{\mathbf{W}}$ equals

$$\tilde{\mathbf{W}} = \hat{\mathbf{H}}_{\text{MMSE}}^H \left(\hat{\mathbf{H}}_{\text{MMSE}} \hat{\mathbf{H}}_{\text{MMSE}}^H + \tilde{\Sigma} + \frac{\sigma_w^2}{E_s} \mathbf{I} \right)^{-1}$$

The matrix $\tilde{\Sigma}$ equals the sum of $M_R \times M_R$ diagonal blocks of Σ , i.e., $\tilde{\Sigma} = \sum_{l=1}^{M_T} \Sigma_{l,l}$ with $\Sigma_{l,l} = (\mathbf{e}_l^T \otimes \mathbf{I}) \Sigma (\mathbf{e}_l \otimes \mathbf{I})$ (here, \mathbf{e}_l is the l th unit vector of length M_T). It is seen that the mismatched and optimal Wiener filter differ by $\tilde{\Sigma}$ which accounts for the additional “noise” caused by the channel estimation errors. The l th element of $\tilde{\mathbf{s}}^{\text{MMSE}}$ equals

$$\tilde{s}_l^{\text{MMSE}} = \tilde{\mu}_l s_l + z_l,$$

where $\tilde{\mu}_l = [\tilde{\mathbf{W}}\hat{\mathbf{H}}_{\text{MMSE}}]_{l,l}$ and z_l captures the residual interference whose power equals $\tilde{\sigma}_l^2 = \tilde{\mu}_l - \tilde{\mu}_l^2$. Assuming that the interference z_l is Gaussian, the *optimal MMSE* demodulator computes the per-layer LLRs

$$\tilde{\Lambda}_{l,i}^{\text{MMSE}} = \frac{1}{\tilde{\sigma}_l^2} \left[\min_{s \in \mathcal{A}_i^0} |\tilde{s}_l^{\text{MMSE}} - \tilde{\mu}_l s|^2 - \min_{s \in \mathcal{A}_i^1} |\tilde{s}_l^{\text{MMSE}} - \tilde{\mu}_l s|^2 \right].$$

4. DEMODULATOR PERFORMANCE

We consider an equivalent “modulation” channel (see Fig. 1) that comprises the space-time modulation, the actual fading channel, and the soft demodulator. The input of this equivalent channel is given by the interleaved code bits d and its output is constituted by the (approximate) LLRs, generically denoted Λ (these LLRs are provided by the genie/mismatched/optimal max-log or MMSE demodulator). We adopt the approach from [3] which proposed to use the mutual information $R \triangleq I(d; \Lambda)$ of the equivalent modulation channel as a *code-independent* performance measure for MIMO soft demodulators. This mutual information can be interpreted as maximum rate that can be achieved with a given demodulator (in the sense of allowing asymptotically error-free communication). A mathematically precise justification of this interpretation was recently provided in [10].

For our setup, it can be shown that (recall that $R_0 = BM_T$)

$$R = R_0 - \frac{1}{2} \sum_{k=1}^{BM_T} \sum_{d_k=0}^1 \int f(\hat{\Lambda}_k|d_k) \log_2 \frac{2f(\hat{\Lambda})}{f(\hat{\Lambda}|d_k)} d\hat{\Lambda}_k, \quad (10)$$

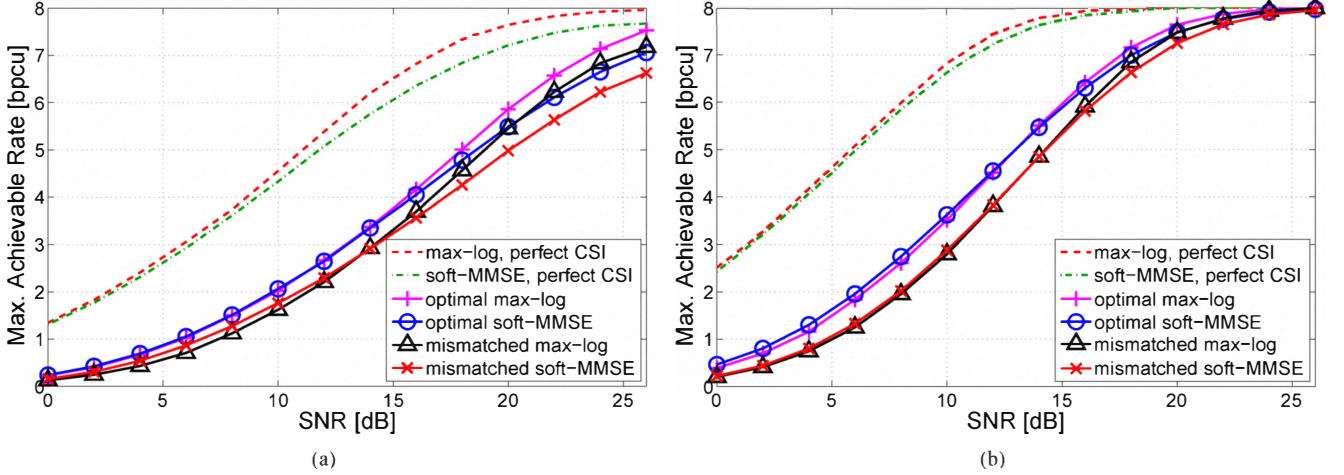


Fig. 2. Comparison of MIMO demodulators for (a) 2×2 and (b) 2×4 uncorrelated MIMO channel.

where $f(\hat{\Lambda}) = \frac{1}{2} \sum_{d_k=0}^1 f(\hat{\Lambda}_k|d_k)$. Analytical expressions for the conditional distributions $f(\Lambda_k|d_k)$ required for calculating the maximum achievable rate are unknown but for rare special cases. Hence, these distributions (and the capacity R) are generally determined numerically via Monte-Carlo simulations.

5. NUMERICAL RESULTS

We next assess the performance of the previously discussed demodulators in terms of the maximum achievable rate in bits per channel use (bpcu). We consider $M_T \times M_R = 2 \times 2$ and 2×4 MIMO-BICM systems with Gray-labeled 16QAM of mean power $E_s = 10$ (here, $R_0 = 8$ bpcu). The pilot power was chosen to be $E_p = 5$. The SNR was varied by changing the noise variance σ_w^2 .

5.1. Capacity for Uncorrelated Channel

Fig. 2 shows the capacity versus SNR for an i.i.d. MIMO channel, i.e., $\mathbf{C}_h = \mathbf{I}$. For both the 2×2 and 2×4 system it is seen that both max-log and MMSE demodulation with imperfect CSI results in significant capacity losses compared to genie max-log and soft MMSE demodulation: at a rate of $R = 4$ bpcu, the SNR gap between the demodulators with perfect CSI and the demodulators with imperfect CSI equals 6 dB (with max-log) and 8 dB (with soft MMSE). However, optimal max-log and MMSE demodulation perform noticeably better than their mismatched counterparts. Specifically, for the 2×2 system shown in Fig. 2(a) the SNR gain of the optimal soft MMSE demodulator over mismatched MMSE ranges from 1 dB at $R = 2$ bpcu to about 1.5 dB at $R = 6$ bpcu. The SNR gain of the optimal max-log demodulator over mismatched max-log is about 1 dB for rates between $R = 2$ and $R = 6$ bpcu. For rates below $R \leq 4$ bpcu soft MMSE demodulation performs identically to or even better than max-log demodulation; at high rates, however, max-log is superior to MMSE demodulation.

Fig. 2(b) shows the results for the 2×4 system. Compared to the 2×2 case, all capacity curves are shifted to lower

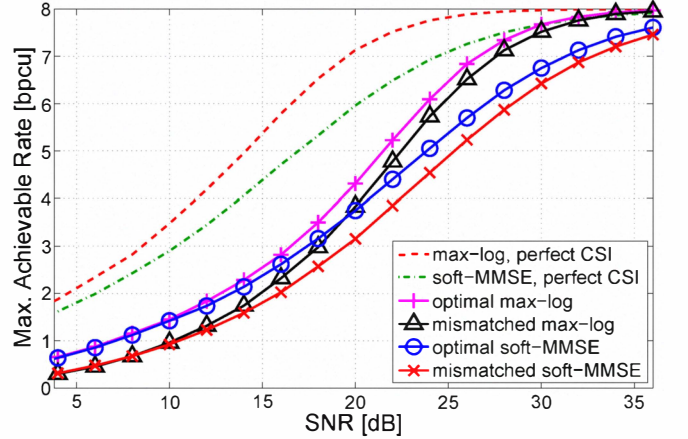


Fig. 3. Comparison of MIMO demodulators for a 2×2 correlated MIMO channel.

SNRs (by about 5 dB at $R = 4$ bpcu), despite the larger number of channel coefficients that have to be estimated (8 complex coefficients instead of 4). Apparently the larger number of receive antennas allows better spatial separation of the two data streams and outweighs the more difficult channel estimation. Max-log and MMSE demodulation (mismatched and optimal) perform almost identically in this scenario, with MMSE having a slight advantage at rates below 4 bpcu. The SNR gain of the optimal demodulators over their mismatched counterparts is about 1.5 dB at medium rates.

5.2. Capacity for Correlated Channel

We next consider the 2×2 system with a correlated MIMO channel that obeys the Kronecker model [11], i.e., $\mathbf{C}_h = \mathbf{T}^{1/2} \otimes \mathbf{R}^{1/2}$. The transmit and receive correlation matrices were chosen as

$$\mathbf{T} = \mathbf{R} = \begin{pmatrix} 1 & \rho \\ \rho & 1 \end{pmatrix}$$

with $\rho = 0.7$. Fig. 3 shows the capacity of the various demodulators versus SNR for this scenario. Compared to the

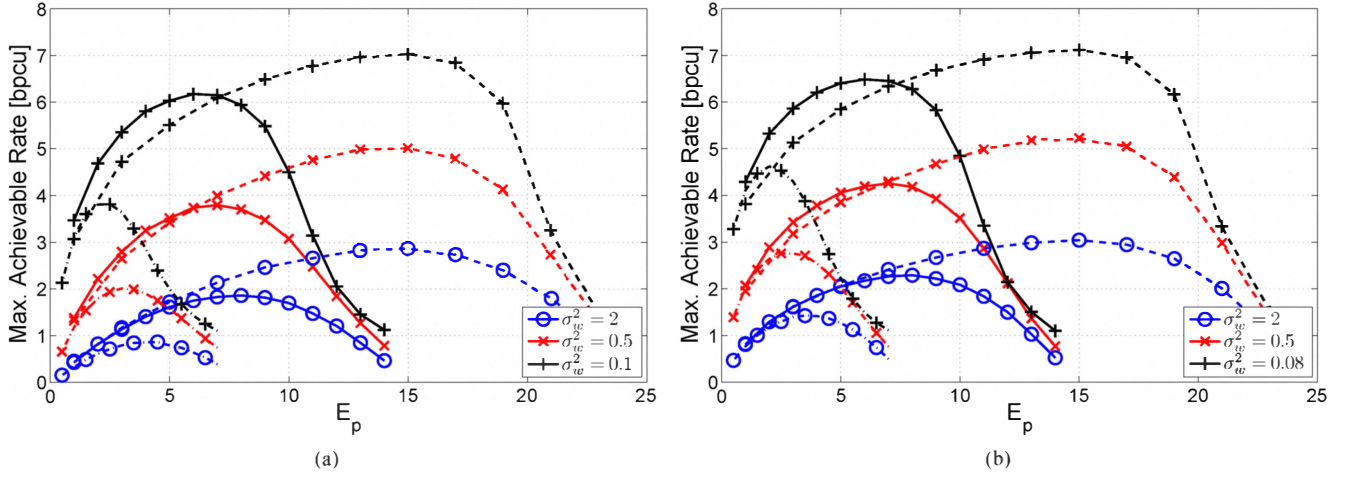


Fig. 4. Impact of pilot power allocation on capacity of (a) mismatched soft MMSE and (b) optimal soft MMSE demodulator for a 2×2 uncorrelated MIMO channel.

uncorrelated case, all curves are shifted to the right by about 4 dB. Furthermore, max-log now outperforms soft MMSE for all rates above 0.5 bpcu: at $R = 4$ bpcu, the gap between optimal max-log and optimal soft MMSE is about 1.5 dB, and in case of the mismatched demodulators the gap is close to 2 dB. Furthermore, optimal max-log and optimal soft MMSE gain 1 dB and 1.5 dB, respectively, over their mismatched counterparts. Apparently, the MMSE equalizer (9) performs worse in case of correlated channels.

5.3. Allocation of Pilot/Data Power

We next fix the total transmit power $E_{\text{tot}} = E_p + E_s$ and study how the allocation of power to pilots (i.e., E_p) and data symbols (i.e., E_s) impacts capacity. We reconsider the 2×2 system with uncorrelated MIMO channel. Fig. 4 shows the results obtained with mismatched (part (a)) and optimal (part (b)) soft MMSE demodulation for total power budgets of $E_{\text{tot}} = 8$ (dash-dotted line), $E_{\text{tot}} = 15$ (solid), $E_{\text{tot}} = 25$ (dashed), and for the three noise levels $\sigma_w^2 = 0.08$ (black '+'), $\sigma_w^2 = 0.5$ (red 'x'), and $\sigma_w^2 = 2$ (blue 'o'). It is seen that the power allocation has a strong impact on capacity: The capacity is very small for low pilot power (due to poor channel estimates) and for high pilot power (due to lack of resources for data transmissions). In between, there is an optimal choice of pilot power, roughly around $E_{\text{tot}}/2$. These results illustrate that improper power allocation can significantly deteriorate the overall performance.

6. CONCLUSION

We studied mismatched and optimal soft MMSE and max-log demodulation in MIMO-BICM system with imperfect CSI. The performance of these demodulators was compared in a code-independent manner in terms of the channel capacity (mutual information) of the equivalent modulation. The optimal demodulators were seen to provide noticeable gains over mismatched demodulation, specifically in the case of uncorrelated MIMO channels. We further observed that optimal pilot power allocation is crucial for achieving optimal performance.

REFERENCES

- [1] A. Guillén i Fàbregas, A. Martinez, and G. Caire, "Bit-Interleaved Coded Modulation," *Foundations and Trends in Communications and Information Theory*, vol. 5, no. 1–2, pp. 1–153, 2008.
- [2] E. Biglieri, G. Taricco, and E. Viterbo, "Bit-interleaved time-space codes for fading channels," in *Proc. Conf. on Information Sciences and Systems*, (Princeton, NJ), pp. WA 4.1–4.6, March 2000.
- [3] P. Fertl, J. Jaldén, and G. Matz, "Capacity-based performance comparison of MIMO-BICM demodulators," in *Proc. IEEE SPAWC-08*, (Recife, Brazil), pp. 166–170, July 2008.
- [4] D. Seethaler, G. Matz, and F. Hlawatsch, "An efficient MMSE-based demodulator for MIMO bit-interleaved coded modulation," in *Proc. IEEE Globecom 2004*, vol. IV, (Dallas, Texas), pp. 2455–2459, Dec. 2004.
- [5] G. Taricco and E. Biglieri, "Space-time decoding with imperfect channel estimation," *IEEE Trans. Wireless Comm.*, vol. 4, no. 4, pp. 1874–1888, 2005.
- [6] S. Sadough, P. Piantanida, and P. Duhamel, "MIMO-OFDM optimal decoding and achievable information rates under imperfect channel estimation," in *Proc. IEEE-SP Workshop on Signal Processing Advances in Wireless Communications*, pp. 1–5, 2007.
- [7] C. Novak, G. Lechner, and G. Matz, "MIMO-BICM with imperfect channel state information: EXIT chart analysis and LDPC code optimization," in *Proc. Asilomar Conf. Signals, Systems, Computers*, (Pacific Grove, CA), pp. 443–447, Oct.–Nov. 2008.
- [8] J. Wang, O. Wen, and S. Li, "Soft-Output MMSE MIMO detector under ML channel estimation and channel correlation," *IEEE Signal Processing Letters*, vol. 16, pp. 667–670, Aug. 2009.
- [9] S. M. Kay, *Fundamentals of Statistical Signal Processing: Estimation Theory*. Englewood Cliffs (NJ): Prentice Hall, 1993.
- [10] J. Jaldén, P. Fertl, and G. Matz, "On the generalized mutual information of BICM Systems with approximate demodulation," in *Proc. IEEE ITW 2010*, (Cairo, Egypt), Jan. 2010.
- [11] C. Oestges, B. Clerckx, D. Vanhoenacker-Janvier, and A. Paulraj, "Impact of fading correlations on MIMO communication systems in geometry-based statistical channel models," *IEEE Trans. Wireless Comm.*, vol. 4, pp. 1112–1120, May 2005.